Design of small-molecule thrombin inhibitors based on the *cis*-5-phenylproline scaffold

K. V. Kudryavtsev,[a] D. A. Shulga,[a] V. I. Chupakhin,[b] A. V. Churakov,[c] N. G. Datsuk,[a] D. V. Zabolotnev,[a] and N. S. Zefirov[a,b]*

[a]*Department of Chemistry, M. V. Lomonosov Moscow State University, Bldg. 3, 1 Leninskie Gory, 119991 Moscow, Russian Federation Fax: +7 (495) 932 8846. E-mail: kudr@org.chem.msu.ru*
[b]*Insitute of Physiologically Active Compounds, Russian Academy of Sciences, 1 Severnyi proezd, 142432 Chernogolovka, Moscow Region, Russian Federation*
[c]*N. S. Kurnakov Institute of General and Inorganic Chemistry, Russian Academy of Sciences, 31 Leninskiy prosp., 119991 Moscow, Russian Federation*

The design of novel organic compounds containing no strongly basic amidine or guanidine functional groups typical of serine protease inhibitors was performed to develop an oral anticoagulant drug. A three-dimensional computational model for thrombin active site was constructed and optimized for docking of small-molecule organic compounds and calculating the energies of inhibitor—enzyme interactions. Novel racemic derivatives of 1-[2-(4-chlorophenylthio)acetyl]-5-phenylpyrrolidine-2,4-dicarboxylic acids were synthesized for which Cl—π interactions between the inhibitors and the S1 pocket of thrombin active site are predicted by modeling. The compounds synthesized deactivate thrombin *in vitro* and the inhibition properties show good correlations with the results of calculations.

Key words: anticoagulant therapy, thrombin, small-molecule inhibitors, molecular docking, 1,3-dipolar cycloaddition, azomethine ylides.

Cardiovascular diseases are the major cause of mortality in modern world. Usually, these pathologies lead to thrombosis which limits the delivery of nutrients and oxygen to tissues and eventually causes cell loss. The final clinical outcomes of blood vessel occlusion include cardiac arrest, acute coronary syndrome, stroke, and peripheral embolism accompanying arterial thrombosis, acute deep vein thrombosis, pulmonary embolism, and paradoxical arterial embolism in the case of vein thrombosis. The reasons for these clinical outcomes include rupture of atherosclerotic plaques, cardiac embolism as a result of fibrillation or left ventricular aneurysm, stasis and immobility in the postoperative period, hypercoagulation states (*e.g.*, protein C deficiency, malignant tumors), and a variety of more rare diseases. In addition, thrombosis is a possible cardiovascular surgery complication and may lead to unstable functioning of implants including artificial heart valves, arterial shunts, and vein filters. Thus, thromboprophylaxis and treatment of thrombosis are key therapeutic goals in the treatment of cardiovascular diseases. Antithrombotic therapy involves the use of drugs that can be divided into three groups with respect to their therapeutic action, *viz.*, anticoagulants inhibiting blood coagulation by influencing the concentration of endogenous thrombin or the enzymatic activity of thrombin; inhibitors of thrombocyte aggregation in hemostasis and thrombosis; and fibrinolytic agents that dissolve the existing thrombi.

A thrombus is formed from a fibrin clot produced as a result of fibrin polymerization under the action of factor XIIIa. In turn, fibrin is formed from fibrinogen under the action of thrombin. Thrombin (factor IIa) is the last-stage enzyme in the complex cascade of biochemical reactions in the blood coagulation system and executes important procoagulant and anticoagulant functions.[1] The use of small-molecule direct thrombin inhibitors is considered as a basic strategy of treatment of various types of thrombosis.[2] At present, anticoagulant therapy in clinical practice involves the use of two small-molecule thrombin inhibitors, *viz.*, parenteral anticoagulant argatroban (**1**) and dabigatran etexilate (**2**) for peroral administration. The latter, also known as Pradaxa™, was approved by the European Commission for prevention of thromboembolic phenomena in elder patients after orthopedic surgery (Spring 2008) and by the U.S. Food and Drug Administration for prevention of strokes in patients with atrial fibrillation (October 2010).[3]

In organism, transformations of dabigatran etexilate (**2**) under the action of enzymes lead to hydrolysis of two functional groups (arrowed) and to the formation of dabigatran, an actual thrombin inhibitor.

Published in Russian in *Izvestiya Akademii Nauk. Seriya Khimicheskaya,* No. 4, pp. 671—679, April, 2011.

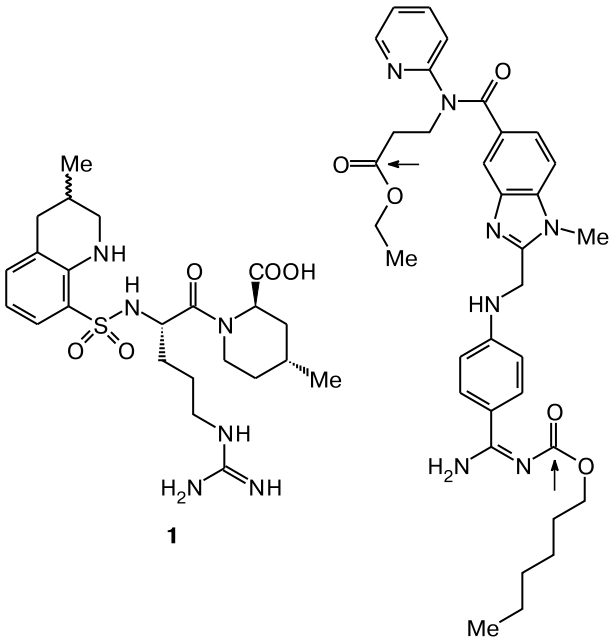

1 **2**

The molecule of human thrombin is comprised of the A-chain (36 amino acid residues) and B-chain (259 amino acid residues) linked by disulfide bridges. Similarly to other serine proteases, thrombin includes a catalytic triad Asp102, His57, and Ser195. A distinctive feature of thrombin is an insertion loop (Tyr60A, Pro60B, Pro60C, Trp60D), which is absent in other serine proteases and restricts access of peptide substrates and inhibitors to the active site. The thrombin active site comprises the catalytic site with nucleophilic Ser195 residue, selective (S1) pocket, large hydrophobic distal (D or S3) pocket, and a small proximal (P or S2) pocket (Fig. 1). The substrate-binding pockets S1, S2, and S3 of the active site interact with the corresponding fragments P1, P2, and P3 of the ligand. The enzyme is highly specific toward peptide hydrolysis after the basic P1 residue (mainly arginine) in which the positively charged guanidine group interacts with the Asp189 residue at the bottom of the S1 pocket. The S2 pocket is formed by the side chains of the Tyr60A and Trp60D residues localized within the insertion loop characteristic of thrombin and mainly binds to hydrophobic amino acids in the P2 position of the substrate. The S3 pocket containing lipophilic and aromatic fragments interacts with the P3 aromatic groups of the ligand. Figure 1 schematically shows the binding of a synthetic tricyclic inhibitor to the thrombin active site[4] according to X-ray data.

Usually, thrombin ligands contain guanidine (argatroban) or amidine (dabigatran) fragment which forms a rather strong bond with the Asp189 residue located in the specific S1 pocket of thrombin active site and determines the strength of the inhibitor—thrombin binding.

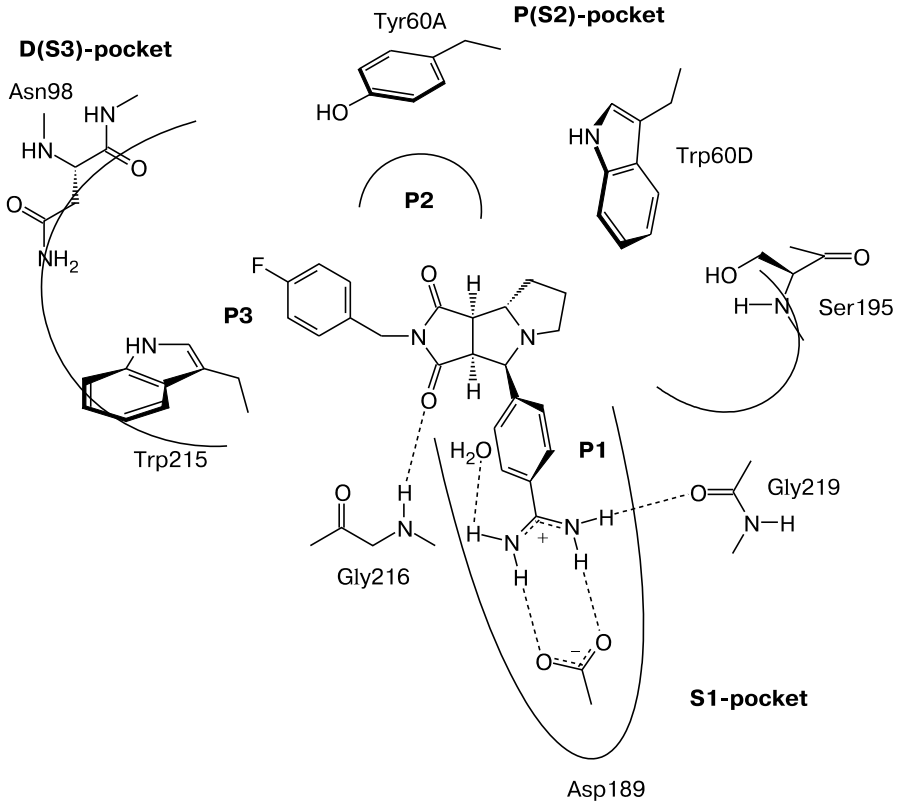

Fig. 1. Binding of tricyclic inhibitor to thrombin active site according to X-ray data[4]: a schematic representation.

However, high basicity of guanidine and amidine groups limit the bioavailability of such drugs. In the case of dabigatran, the bioavailability is enhanced by conversion of the inhibitor to a double prodrug, dabigatran etexilate. Recent studies have demonstrated that the P1 fragment of the inhibitor should not necessarily contain a functional group of high basicity (*e.g.*, guanidine or amidine) for efficient inhibition of thrombin. X-ray studies of some inhibitors revealed a deep insertion of the chlorophenyl fragment of the inhibitor molecule into the S1 pocket of thrombin active site. In addition to complementary hydrophobic interactions, studies of tripeptidomimetic **3** (it inhibits thrombin through unusual electrostatic interactions and entropy factors) and some other compounds revealed location of the chlorine atom near the aromatic ring of the side chain of the Tyr228 residue of thrombin.[5]

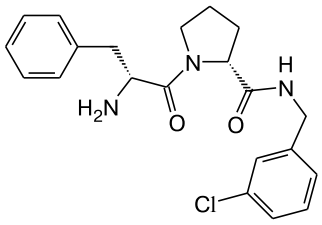

3

The contribution of such a Cl—π interaction to the total energy of the inhibitor—enzyme interaction can be as large as 8.4 kJ mol^{-1},[6] and may be considered as a promising feature for an increase in the thrombin affinity of the compounds being designed. The aim of the present work was to design small-molecule thrombin inhibitors with low basicity using the conformationally rigid *cis*-5-phenylproline scaffold and methods of computer simulation of ligand—thrombin interactions.

The new molecular scaffold for the design of thrombin inhibitors includes (Scheme 1) derivatives of 5-arylpyrrolidine-2,4-dicarboxylic acids **5** which can be obtained with ease by 1,3-dipolar cycloaddition of *tert*-butyl acrylate to azomethine ylides generated from imino esters **4**.[7]

Conformational rigidity of the central pyrrolidine ring and the exactly determined spatial arrangement of substituents[7] in compounds **5** facilitates the simulation and reduces the entropy factors of the interaction with biological targets. Also, this molecular scaffold was chosen based on the available data on the thrombin-inhibiting properties of small-molecule compounds containing the structural fragment **5**.[8] To check the possibility of design of thrombin inhibitors with low basicity, we planned to convert pyrrolidine-2,4-dicarboxylic acid derivatives **5** to polysubstituted pyrrolidines **6** and **7** (see Scheme 1) in which the 4-chlorophenylsulfanyl fragment should be the P1 frag-

Scheme 1

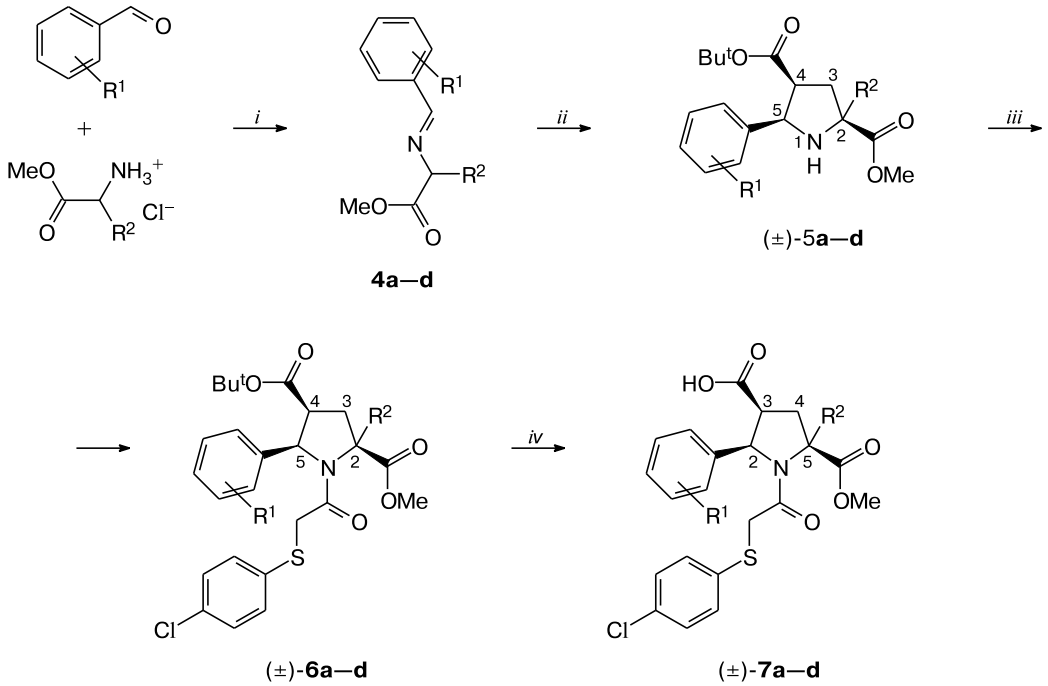

$R^1 = R^2 = H$ (**a**); R^1 = 4-Br, $R^2 = H$ (**b**); $R^1 = H$, R^2 = Me (**c**); R^1 = 2-MeO, R^2 = Me (**d**)

i. Et_3N, $MgSO_4$, CH_2Cl_2; *ii*. *tert*-butyl acrylate, LiBr, Et_3N, THF; *iii*. 1) $ClCH_2COCl$, Et_3N, THF; 2) 4-ClPhSH, DMF, K_2CO_3; *iv*. HCl, ether.

ment of the ligand and interact with the S1 pocket of thrombin active site. The substituents R^1 and R^2 were chosen taking into account the availability of the starting reactants and the need to assess how structural factors influence the biological activity.

A computer model for thrombin active site was constructed using the X-ray data[5] for a complex of thrombin with tripeptidomimetic **3**. To carry out molecular docking, water molecules were removed from the protein structure and hydrogen atoms were added to all amino acid residues. The molecular structures of compounds **6** and **7** were optimized using the MMFF94 force field[9] (within the framework of the OpenBabel program[10]) and then preprocessed by the AutoDockTools software.[11] Since we planned to synthesize some racemic derivatives (see Scheme 1), calculations of the ligand—thrombin interaction were performed for both enantiomeric series. The most energetically favorable conformations of the pyrrolidines **6** and **7** are the enantiomeric structures labeled "**I**" and "**IV**". Calculations were carried out taking into account not only the differences in the interaction of the enantiomers with the chiral environment of the thrombin active site, but also possible conformers labeled "**II**" and "**III**", which differ from the structures **I** and **IV** in position of the amide bond.

Correctness of the thrombin active site model thus constructed was confirmed by the results of docking of the structure of tripeptidomimetic **3**. The calculated conformation of compound **3** and its arrangement in the thrombin active site were in excellent agreement with the crystallographic data.[5] According to our calculations, the energy of the **3**—thrombin interaction (AutoDock 4.2) is -29.7 kJ mol^{-1} (K_i = 6250 nmol L^{-1}), being 8.8 kJ mol^{-1} higher than the experimental value -38.5 kJ mol^{-1} (K_i = 180±140 nmol L^{-1}).[5] The parameterization of the AutoDock software does not include the Cl—π interactions[6] in explicit form, and in our model the key role is seemingly played by the hydrophobic interactions and the shape match of the chlorophenyl fragment of the inhibitor and the S1 pocket of thrombin active site.

Ligand-protein Cl—π interactions are typical of the crystal structures;[6] however, the known molecular modeling software does not include them in explicit form. In this connection, the development of methods for taking into account these interactions in molecular docking and virtual screening software seems to be promising. There are grounds to believe that if the structure of the ligand—thrombin complex obtained from docking matches the available crystal structure (PDB : 2ZC9), one can expect an additional stabilization energy of these binding modes through the Cl—π interactions ignored by the AutoDock4.2 software. For most conformers of the polysubstituted pyrrolidines **6** and **7** presented here, calculations predict the highest stability for such modes in which the 4-chlorophenyl fragment of the small-molecule compound is within the S1 pocket of thrombin active site. Also, often the coordinates of the 4-chlorophenyl fragment of compounds **6** and **7** in the thrombin active site are close to the crystallographic coordinates of the 3-chlorophenyl fragment of ligand **3** in the complex PDB : 2ZC9. This can be explained by good shape match of the chlorophenyl fragment and the rather narrow S1 pocket. According to docking results, the highest thrombin affinity has structure **6c(III)** (Fig. 2, *a*; Table 1) in which the ligand shape almost perfectly matches that of the S1 pocket and the 4-chlorophenyl fragment is in the S1 pocket and directed at the hydroxybenzyl side chain of the Tyr228 residue at the bottom of the pocket. The 5-phenyl substituent in the central pyrrolidine fragment of **6c(III)** is directed at the S2 pocket between the aromatic side chains

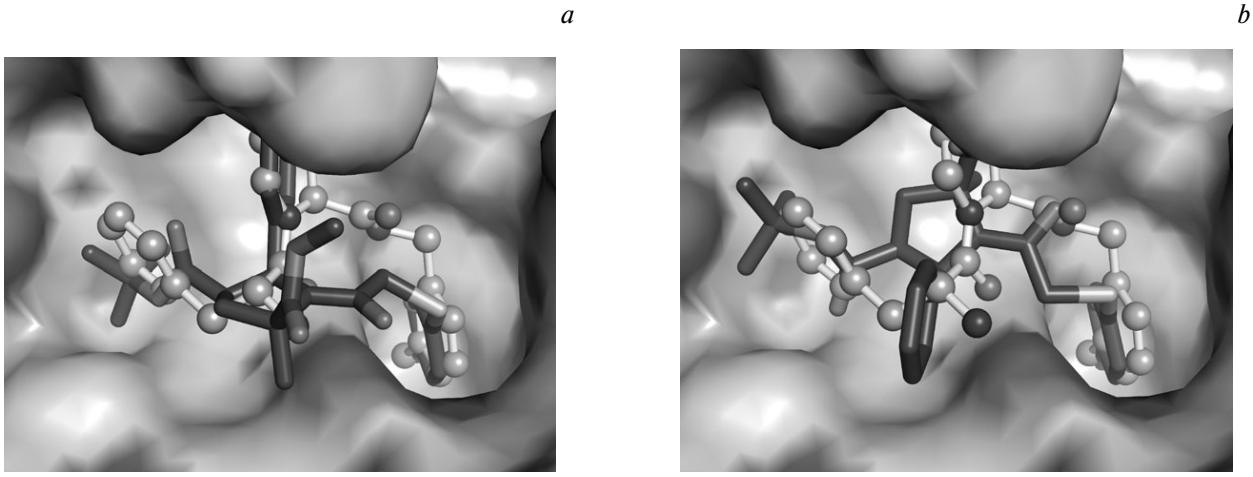

Fig. 2. The most energetically favorable interactions of enantiomers (2*R*,4*R*,5*S*)-**6c** (*a*) and (2*S*,4*S*,5*R*)-**6c** (*b*) with thrombin active site predicted by molecular docking. Inhibitor **3** is shown in ball-and-stick view and the enantiomers of the *N*-(2-(4-chlorophenylthio)acetyl)-5-phenylpyrrolidine-2,4-dicarboxylic acid derivative **6c** are shown in thick stick view.

of the Tyr60A and Trp60D residues (see Fig. 2, *a*). The S atom of the 4-chlorophenylsulfanyl fragment in conformer **6c(III)** is near the Cys191—Cys220 disulfide bond (5.6 and 4.5 Å, respectively), which can lead to energetically favorable van der Waals interactions. According to calculations, in most conformers mentioned above the S3 pocket of the thrombin active site is filled with the *tert*-butoxycarbonyl group (for enantiomers (2*R*,4*R*,5*S*)-**6**) or 5-phenyl substituent (for (2*S*,4*S*,5*R*)-**6** and (2*S*,4*S*,5*R*)-**7**). Further optimization of the inhibitors may lead to addi-

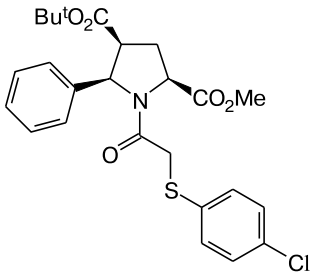

6a(I)

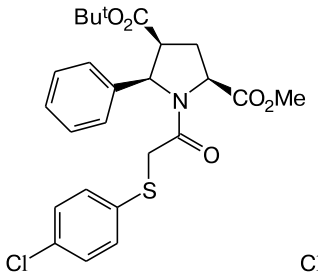

6a(II)

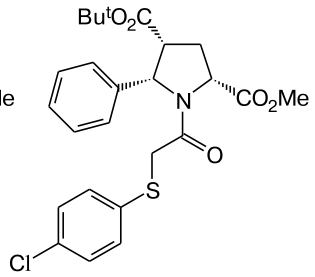

6a(III)

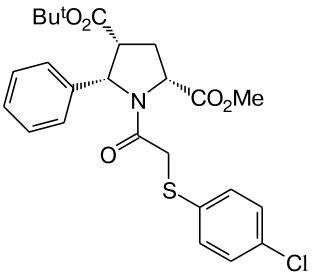

6a(IV)

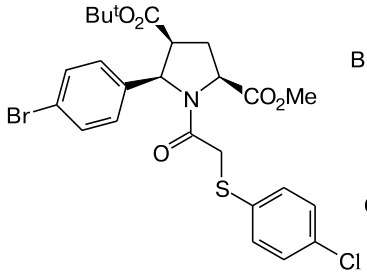

6b(I)

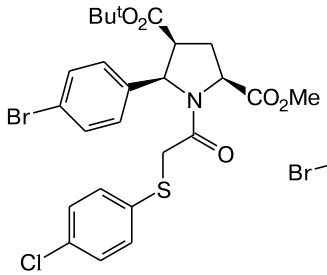

6b(II)

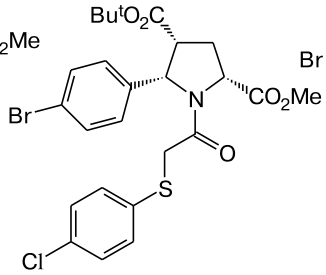

6b(III)

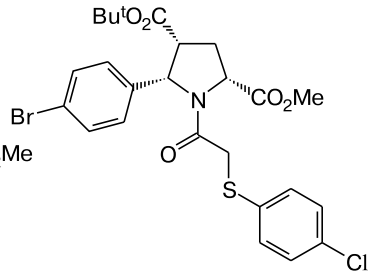

6b(IV)

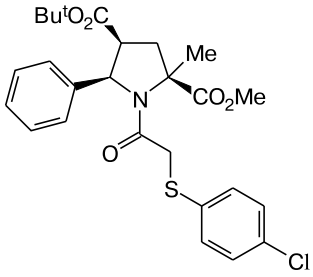

6c(I)

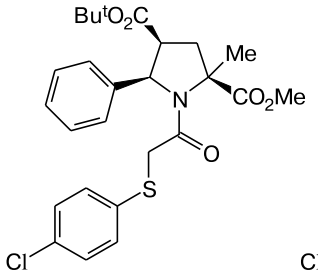

6c(II)

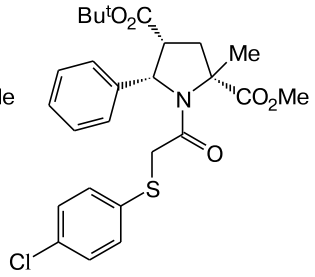

6c(III)

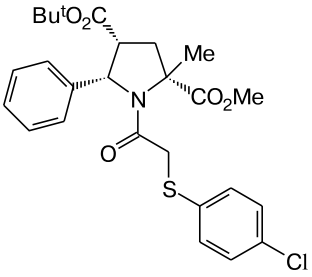

6c(IV)

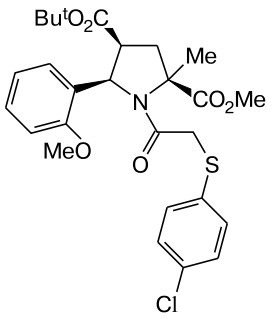

6d(I)

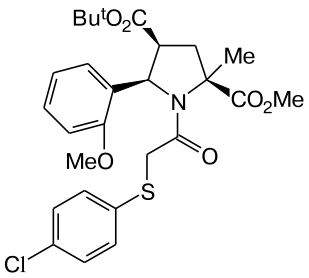

6d(II)

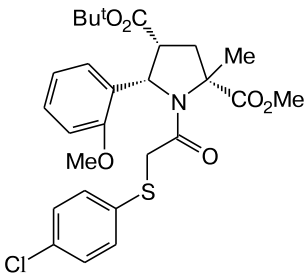

6d(III)

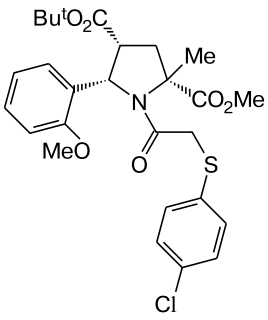

6d(IV)

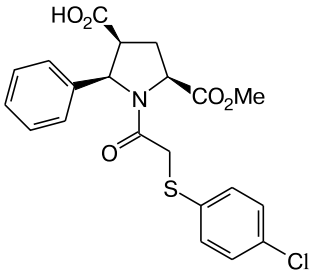

7a(I)

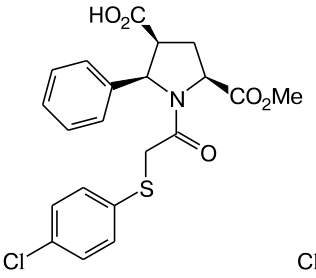

7a(II)

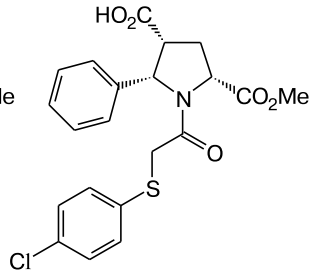

7a(III)

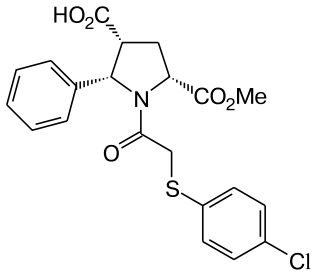

7a(IV)

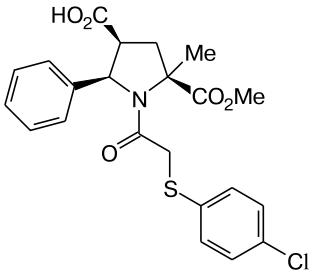

7c(I)

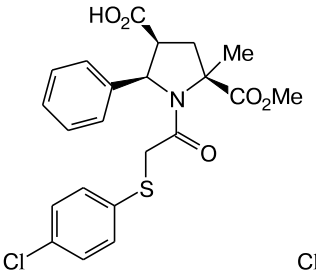

7c(II)

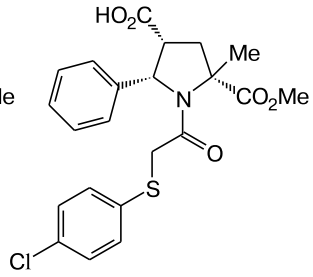

7c(III)

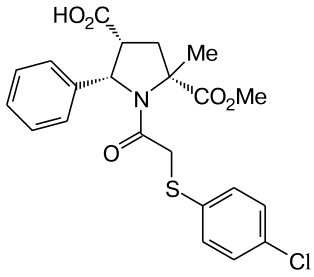

7c(IV)

tional strengthening of interactions in this region owing to the larger contact area and to more specific interactions with the Asn98 residue. According to calculations, some interactions of thrombin with polysubstituted pyrrolidines **6** and **7** which are characterized by higher energies correspond to localization of the 4-chlorophenylsulfanyl fragment of the inhibitor in the distal S3 pocket of thrombin active site. This interaction may be the starting point of a molecular recognition process resulting in a more stable complex with the filled S1 pocket. A post-docking analysis of the geometries of the complexes of polysubstituted pyrrolidines **6** and **7** with thrombin suggests that the *cis*-5-proline molecular scaffold allows permits efficient filling of the S1 and S3 pockets of thrombin active site. The interaction of inhibitors with the S2 pocket of thrombin active site is an important factor for the selectivity of the compounds being designed toward related trypsin proteases. Docking of structure **6b(III)** involves a complementary filling of the S2 pocket of the 5-(4-bromophenyl) substituent, and a halogen bonding[12] with polar heteroatoms of the His57 and Lys60F residues becomes possible. According to docking results for enantiomeric structure **6b(I)**, the interaction involves the S1 and S3 pockets of thrombin active site, whereas the S2 pocket remains unfilled. One can assume that the design of thrombin inhibitors based on the (2*S*,4*S*,5*R*)-**5** molecular scaffold will result in compounds with low selectivity toward trypsin. Docking showed that *ortho*-substitution of the 5-phenyl fragment

Table 1. Inhibition of thrombin by *N*-[2-(4-chlorophenylthio)acetyl]-5-phenylpyrrolidine-2,4-dicarboxylic acid derivatives in buffer solution and calculated thrombin-inhibiting ability[a]

Compound	*M*	*E*/kJ mol^{-1}				K_i/μmol L^{-1}				I_{max} (%) (c/μmol L^{-1})
		I	II	III	IV	I	II	III	IV	
6a	490.02	−23.7	−25.2	−25.0	−27.2	71	37	41	18	—[b]
6b	568.92	−26.5	−25.5	−26.7	−25.6	23	35	22	33	—[b]
6c	504.05	−24.3	−25.7	−27.2	−21.4	56	31	17	182	53 (180)
6d	534.08	−23.6	−21.9	−21.2	−20.6	74	145	193	245	—[b]
7a	433.91	−26.7	−24.3	−24.0	−26.0	21	56	63	28	51 (4300)
7c	447.94	−25.8	−23.9	−24.5	−25.0	31	66	53	41	27 (400)

[a] *M* is the molecular weight of inhibitor. *E* is the calculated energy of the interaction with thrombin conformers (I—IV). K_i is the calculated constant of thrombin inhibition by the conformers **I—IV**; I_{max} is the maximum inhibition of thrombin in the buffer solution.

[b] Not measured.

in (2*R*,4*R*,5*S*)-**6d** leads to violation of the shape correspondence between the molecular fragments of the inhibitor and the specific protein pockets. The stronger binding was predicted for the enantiomeric structure **6d(I)** (74 μmol L^{-1}) in which the 5-(2-methoxyphenyl) fragment molecule interacts with the S3 pocket of thrombin active site. Thus, an important feature of our model for thrombin active site and the docking protocol is differentiation of chiral small-molecule organic compounds.

To experimentally check the predicted interactions, we synthesized novel 5-phenylpyrrolidine-2,4-dicarboxylic acid derivatives **6** and **7** (see Scheme 1). The cycloaddition of *tert*-butyl acrylate to azomethine ylides generated from imino esters **4** under the action of Lewis acids proceeds stereospecifically to give the racemic pyrrolidine **5** in which both carboxyl groups and the 5-phenyl substituent are on the one side of the pyrrolidine ring (see Scheme 1).[7] Further synthetic modifications of the molecular scaffold **5** involving the introduction of the 2-(4-chlorophenylthio)acetyl substituent at the endocyclic atom of the pyrrolidine ring and resulting in compounds **6** do not involve stereogenic centers. Nevertheless, to exactly determine the molecular structure of this class of compounds, we carried out an X-ray study of crystals of the polysubstituted pyrrolidine **6d** (Fig. 3, Table 2). The crystal studied belonged to the space group $P2_12_12_1$ which includes only three symmetry elements, *viz.*, the translational axes 2_1 passing along three mutually perpendicular directions. Therefore, the crystal structure of pyrrolidine **6d** has no symmetry elements that transform one molecular configuration to a mirror molecular configuration. According to X-ray data, the unit cell of compound **6d** in the crystal contains only one independent molecule, *i.e.*, crystallization led to

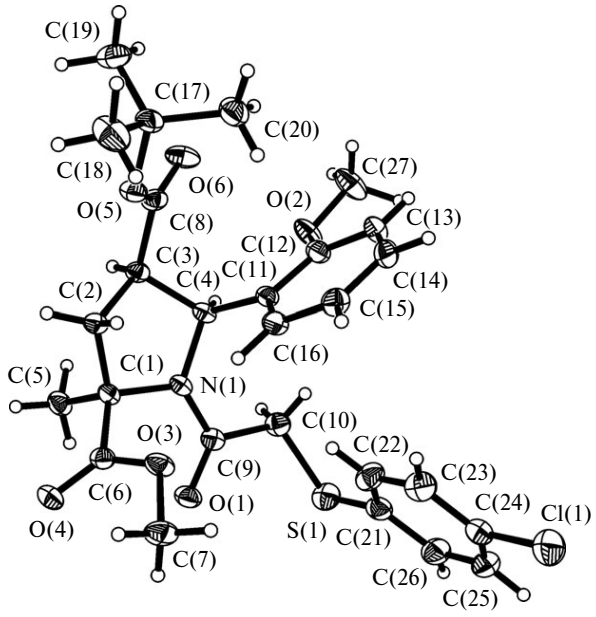

Fig. 3. Molecular structure of compound **6d**.

Table 2. Selected bond lengths (*d*/Å) and bond angles (ω/deg) in molecule of (2*R*,4*R*,5*S*)-**6d**

Bond	*d*/Å	Angle	ω/deg
S(1)—C(21)	1.7574(16)	C(21)—S(1)—C(10)	103.01(7)
S(1)—C(10)	1.7968(14)	C(9)—N(1)—C(1)	119.02(10)
Cl(1)—C(24)	1.7431(16)	C(9)—N(1)—C(4)	126.68(11)
N(1)—C(9)	1.3495(17)	C(1)—N(1)—C(4)	113.66(10)
N(1)—C(1)	1.4751(16)	C(6)—O(3)—C(7)	114.95(11)
N(1)—C(4)	1.4814(15)	N(1)—C(1)—C(5)	111.29(11)
O(1)—C(9)	1.2266(16)	N(1)—C(1)—C(6)	111.03(10)
O(2)—C(12)	1.3615(17)	C(5)—C(1)—C(6)	109.53(11)
O(2)—C(27)	1.4204(17)	N(1)—C(1)—C(2)	102.04(10)
O(3)—C(6)	1.3340(17)	C(5)—C(1)—C(2)	111.83(11)
O(3)—C(7)	1.4511(16)	C(6)—C(1)—C(2)	110.96(10)
O(4)—C(6)	1.1984(16)	C(3)—C(2)—C(1)	102.85(10)
O(5)—C(8)	1.3317(16)	C(8)—C(3)—C(2)	116.88(11)
O(5)—C(17)	1.4885(16)	C(8)—C(3)—C(4)	111.69(10)
O(6)—C(8)	1.2062(16)	C(2)—C(3)—C(4)	104.42(10)
C(1)—C(5)	1.5303(18)	N(1)—C(4)—C(11)	113.24(10)
C(1)—C(6)	1.5314(17)	N(1)—C(4)—C(3)	101.76(10)
C(1)—C(2)	1.5400(18)	C(11)—C(4)—C(3)	112.61(10)
C(2)—C(3)	1.5305(17)	O(3)—C(6)—C(1)	112.53(11)
C(3)—C(8)	1.5168(18)	O(5)—C(8)—C(3)	111.63(11)
C(3)—C(4)	1.5593(18)	O(1)—C(9)—N(1)	121.10(12)
C(4)—C(11)	1.5220(17)	O(1)—C(9)—C(10)	122.24(12)
C(9)—C(10)	1.5257(19)	N(1)—C(9)—C(10)	116.64(11)

separation of enantiomers. The absolute configuration of molecules **6d** constituting the crystal under study was exactly determined owing to the presence of heavy atoms (sulfur and chlorine, see Fig. 3). Spontaneous separation of enantiomers of the derivatives of *N*-(4-chlorophenylthio)acetyl-5-phenylpyrrolidine-2,4-dicarboxylic acids **6** under crystallization will be used in further studies to obtain enantiomerically pure thrombin inhibitors based on the molecular scaffold **5**. The inhibiting properties of the compounds synthesized were tested taking hydrolysis of a thrombin substrate in a buffer solution in the presence of thrombin (see the rightmost column in Table 1)*. All the three compounds studied (**6c**, **7a**, **7c**) appeared to be thrombin inhibitors. The enzymatic activity of thrombin is more than halved in the presence of polysubstituted pyrrolidine **6c** at a concentration of 180 μmol L^{-1} (see Table 1). This experimentally determined value agrees well with the calculated values of the constant of thrombin inhibition by compound **6c**, which lies in the range 17—182 μmol L^{-1} (see Table 1). This suggests a high predictive power of the constructed model for thrombin active site and the docking protocol.

* Tested at the Physical Biochemistry Laboratory (Hematology Research Center, Ministry of Health and Social Development of the Russian Federation, Moscow, Russia) headed by Prof. F. I. Ataullakhanov.

Summing up, a combination of a molecular docking study and analysis of ligand-protein interactions followed by multistage targeted syntheses and biochemical studies gave a series of novel nonbasic small-molecule organic compounds based on the *cis*-5-phenylproline molecular scaffold. These compounds exhibit inhibiting properties toward thrombin, the key serine protease for hemostasis.

Experimental

Molecular docking was carried out individually for each structure on the SKIF—MSU "Chebyshev" supercomputer cluster facilities using the AutoDock4.2 software.[11]

Compounds used in the experiments include *tert*-butyl acrylate, aromatic aldehydes, chloroacetyl chloride, 4-chlorothiophenol, and silica gel (Lancaster). Prior to use, benzaldehyde was purified by distillation *in vacuo*. The course of reactions and the purity of the compounds was monitored using Sorbfil PTSKh-AF-A-UF TLC plates with $CHCl_3$—MeOH (10 : 1) as eluent.

^1H and ^{13}C NMR spectra were recorded on a Bruker Avance 400 instrument (operating frequency is 400 MHz for ^1H and 100 MHz for ^{13}C) at T = 303 K in solutions in DMSO-d_6 or $CDCl_3$ using the residual solvent signals as internal standards. An X-ray study of compound **6d** was carried out on a Bruker SMART APEX II automated diffractometer at 150.0(2) K (Mo-Kα radiation, λ = 0.71073 Å, graphite monochromator). The structure was solved by the direct methods and refined using the full-matrix least-squares method with respect to F^2 in the anisotropic approximations for all non-hydrogen atoms.[13] All hydrogen atoms were located objectively and refined isotropically.

The effect of compounds **6c**, **7a**, and **7c** on the enzymatic activity of thrombin was studied photometrically.[14]

Diesters of pyrrolidine-2,4-dicarboxylic acids **5a**,[15] **5b**,[8] and **5c** (see Ref. 7) were synthesized from imino esters **4a**—**c** following the known procedures and identified spectroscopically. Imino ester **4d** was synthesized by a known procedure.[16] Compound **5d** was obtained from imino ester **4d** and *tert*-butyl acrylate, as described for structural analogs.[7]

Methyl 2-(2-methoxybenzilidenamino)propanoate (4d) was synthesized from DL-alanine methyl ester hydrochloride and 2-methoxybenzaldehyde and used in the subsequent stage without additional purification. The yield was 89%. An oily substance. ^1H NMR (DMSO-d_6, δ, J/Hz): 1.37 (d, 3 H, CH_3, J = 6.8); 3.64 (s, 3 H, OCH_3); 3.86 (s, 3 H, $COOCH_3$); 4.24 (q, 1 H, H(2), J = 6.8); 6.99 (t, 1 H_{arom}, J = 7.5); 7.11 (d, 1 H_{arom}, J = 8.0); 7.44—7.49 (m, 1 H_{arom}); 7.82 (d, 1 H_{arom}, J = 7.5); 8.70 (s, 1 H, CH=).

(2*S,4*S**,5*R**)-4-*tert*-Butoxycarbonyl-2-methoxycarbonyl-5-(2-methoxyphenyl)-2-methylpyrrolidine (5d).** Obtained from compound **4d** and *tert*-butyl acrylate. The yield was 81%. Colorless crystals, m.p. 73—74 °C. ^1H NMR ($CDCl_3$, δ, J/Hz): 0.98 (s, 9 H, $(CH_3)_3$); 1.50 (s, 3 H, 2-CH_3); 2.06 (dd, 1 H, H(3), J = 13.6, J = 8.1); 2.60 (dd, 1 H, H(3), J = 13.6, J = 3.5); 3.43—3.48 (m, 1 H, H(4)); 3.81 (s, 3 H, OCH_3); 3.85 (s, 3 H, $COOCH_3$); 4.71 (d, 1 H, H(5), J = 7.1); 6.85 (d, 1 H_{arom}, J = 8.1); 6.92 (d, 1 H_{arom}, J = 7.5); 7.20—7.25 (m, 1 H_{arom}); 7.32 (d, 1 H_{arom}, J = 7.5). ^{13}C NMR ($CDCl_3$, δ): 27.03, 27.46 (3 C), 41.65, 49.07, 52.44, 55.18, 59.72, 65.10, 79.90, 109.80, 120.29, 126.43, 126.83, 128.19, 157.04, 172.59, 176.48. Found (%): C, 65.43; H, 7.71; N, 3.89. $C_{19}H_{27}NO_5$. Calculated (%): C, 65.31; H, 7.79; N, 4.01.

Synthesis of 5-aryl-1-[2-(4-chlorophenylthio)acetyl]pyrrolidine-2,4-dicarboxylic acid esters 6a-d (general procedure). To a solution of pyrrolidine-2,4-dicarboxylic acid diester **5** (20 mmol) in THF (50 mL), Et_3N (2.63 g, 26 mmol, 3.63 mL) was added in argon atmosphere. The reaction mixture was cooled and a solution of chloroacetyl chloride (2.71 g, 24 mmol, 1.91 mL) in THF (20 mL) was added with stirring at such a rate that the temperature was at most +5 °C. The mixture was stirred for 5 h at room temperature and the Et_3N·HCl residue was filtered off. The filtrate was concentrated *in vacuo* with a rotary evaporator. The residue (*N*-chloroacetyl derivative of compound **5**) was dissolved in DMF (120 mL) in argon atmosphere. To this solution, K_2CO_3 (2.76 g, 20 mmol) was added and a solution of 4-chlorothiophenol (2.90 g, 20 mmol) in DMF (40 mL) was added on stirring. The combined solution was stirred for 24 h at room temperature; then, DMF was evaporated *in vacuo*. Water (60 mL) and 1 *M* NaOH (60 mL) was added and extracted with EtOAc (3×60 mL). The combined organic extracts were washed with saturated NaCl solution (20 mL) and dried with Na_2SO_4. The drying agent was filtered off and the filtrate was concentrated *in vacuo* with a rotary evaporator. The residue was chromatographed on 60 silica gel (Lancaster, particle size 0.040—0.063 mm) using $CHCl_3$—MeOH (20 : 1) as eluent.

(2*S,4*S**,5*R**)-4-*tert*-Butoxycarbonyl-1-[2-(4-chlorophenylthio)acetyl]-2-methoxycarbonyl-5-phenylpyrrolidine (6a).** The yield was 65%, colorless crystals, m.p. 135 °C. ^1H NMR ($CDCl_3$, δ, J/Hz): 1.14 (s, 9 H, $(CH_3)_3$); 2.35—2.42 (m, 1 H, H(3)); 2.48—2.58 (m, 1 H, H(3)); 3.37 (s, 2 H, CH_2S); 3.40—3.48 (m, 1 H, H(4)); 3.84 (s, 3 H, $COOCH_3$); 4.41 (dd, 1 H, H(2), J = 11.4, J = 6.8); 5.30 (d, 1 H, H(5), J = 9.1); 7.20—7.26 (m, 4 H_{arom}); 7.32—7.38 (m, 3 H_{arom}); 7.61 (d, 2 H_{arom}, J = 6.8). ^{13}C NMR ($CDCl_3$, δ): 27.62 (3 C), 28.91, 36.98, 50.53, 52.46, 59.69, 63.29, 81.83, 128.34 (2 C), 128.64, 128.72 (2 C), 129.10 (2 C), 131.20 (2 C), 132.90, 133.39, 137.61, 167.53, 167.63, 171.87. Found (%): C, 61.25; H, 5.92; N, 2.99. $C_{25}H_{28}ClNO_5S$. Calculated (%): C, 61.28; H, 5.76; N, 2.86.

(2*S,4*S**,5*R**)-5-(4-Bromophenyl)-4-*tert*-butoxycarbonyl-1-[2-(4-chlorophenylthio)acetyl]-2-methoxycarbonylpyrrolidine (6b).** The yield was 71%, colorless crystals, m.p. 124—125 °C. ^1H MR ($CDCl_3$, δ, J/Hz): 1.18 (s, 9 H, $(CH_3)_3$); 2.34—2.49 (m, 2 H, H(3)); 3.29—3.37 (m, 2 H, CH_2S); 3.42 (ddd, 1 H, H(4), J = 12.7, J = 8.6, J = 6.8); 3.83 (s, 3 H, $COOCH_3$); 4.41 (dd, 1 H, H(2), J = 11.1, J = 7.1); 5.26 (d, 1 H, H(5), J = 8.6); 7.22—7.27 (m, 4 H_{arom}); 7.47—7.52 (m, 4 H_{arom}). ^{13}C NMR ($CDCl_3$, δ): 27.70 (3 C), 28.81, 37.12, 50.46, 52.54, 59.64, 62.63, 82.13, 122.82, 129.17 (2 C), 130.00 (2 C), 131.61 (2 C), 131.82 (2 C), 133.04, 133.26, 136.69, 167.33, 167.56, 171.90. Found (%): C, 52.89; H, 4.82; N, 2.39. $C_{25}H_{27}BrClNO_5S$. Calculated (%): C, 52.78; H, 4.78; N, 2.46.

(2*S,4*S**,5*R**)-4-*tert*-Butoxycarbonyl-1-[2-(4-chlorophenylthio)acetyl]-2-methoxycarbonyl-2-methyl-5-phenylpyrrolidine (6c).** The yield was 72%, colorless crystals, m.p. 73—74 °C. ^1H NMR ($CDCl_3$, δ, J/Hz): 1.11 (s, 9 H, $(CH_3)_3$); 1.55 (s, 3 H, 2-CH_3); 1.99 (dd, 1 H, H(3), J = 12.8, J = 6.4); 2.77 (t, 1 H, H(3), J = 13.3); 3.23 (s, 2 H, CH_2S); 3.66 (ddd, 1 H, H(4), J = 13.3, J = 9.3, J = 6.4); 3.82 (s, 3 H, $COOCH_3$); 5.38 (d, 1 H, H(5), J = 9.3); 7.22 (s, 4 H_{arom}); 7.30—7.39 (m, 3 H_{arom}); 7.64 (d, 2 H_{arom}, J = 6.8). ^{13}C NMR ($CDCl_3$, δ): 20.49, 27.56 (3 C), 36.98, 37.60, 49.45, 52.66, 63.22, 66.41, 81.75, 128.45 (2 C),

128.61 (2 C), 128.76 (2 C), 129.06 (2 C), 131.44 (2 C), 133.10, 138.16, 166.61, 167.88, 173.47. Found (%): C, 62.25; H, 5.93; N, 2.98. $C_{26}H_{30}ClNO_5S$. Calculated (%): C, 61.96; H, 6.00; N, 2.78.

(2*S,4*S**,5*R**)-4-*tert*-Butoxycarbonyl-1-[2-(4-chlorophenylthio)acetyl]-2-methoxycarbonyl-5-(2-methoxyphenyl)-2-methylpyrrolidine (6d).** The yield was 68%, colorless crystals, m.p. 153—154 °C. ^{1}H NMR ($CDCl_3$, δ, *J*/Hz): 1.08 (s, 9 H, $(CH_3)_3$); 1.56 (s, 3 H, 2-CH_3); 2.03 (dd, 1 H, H(3), *J* = 12.8, *J* = 6.7); 2.82 (t, 1 H, H(3), *J* = 13.1); 3.20 (d, 1 H, CH_2S, *J* = 14.6); 3.31 (d, 1 H, CH_2S, *J* = 14.6); 3.66 (ddd, 1 H, H(4), *J* = 13.1, *J* = 9.5, *J* = 6.7); 3.80 (s, 3 H, OCH_3); 3.84 (s, 3 H, $COOCH_3$); 6.00 (d, 1 H, H(5), *J* = 9.5); 6.84 (d, 1 H_{arom}, *J* = 8.3); 7.02 (d, 1 H_{arom}, *J* = 7.5); 7.17—7.21 (m, 4 H_{arom}); 7.26—7.30 (m, 1 H_{arom}); 7.96 (dd, 1 H_{arom}, *J* = 7.5, *J* = 1.6). ^{13}C NMR ($CDCl_3$, δ): 20.50, 27.38 (3 C), 37.17, 38.03, 48.80, 52.60, 54.82, 55.33, 66.16, 81.12, 109.92, 121.41, 126.99, 128.91 (2 C), 129.52 (2 C), 130.90 (2 C), 132.50, 133.90, 156.37, 166.59, 168.22, 173.50. Found (%): C, 61.01; H, 5.91; N, 2.89. $C_{27}H_{32}ClNO_6S$. Calculated (%): C, 60.72; H, 6.04; N, 2.62.

X-ray study of compound 6d. A crystal (dimensions 0.25×0.20×0.15 mm) was grown by slow evaporation of solvents from a dilute solution of **6d** in a hexane—AcOEt (1 : 1) mixture. Crystals of (2*R*,4*R*,5*S*)-**6d** ($C_{27}H_{32}Cl_1N_1O_6S_1$, M = 534.05) are orthorhombic, space group $P2_12_12_1$, *a* = 10.1984(5), *b* = = 13.1163(6), *c* = 19.9614(9) Å, *V* = 2670.1(2) Å^3, *Z* = 4, d_{calc} = 1.328 g cm^{-3}, μ(Mo-Kα) = 0.263 mm^{-1}, and *F*(000) = = 1128. The intensities of 27808 reflections (6549 independent reflections, R_{int} = 0.0310) were measured using ω-scan with a 0.5° increment in the interval $2.24 < \theta < 28.00°$ ($-13 \le h \le 13$, $-17 \le k \le 17$, $-26 \le l \le 26$). The final reliability factor was $R_1 = 0.0289$, $R_w = 0.0732$ for 6094 reflections with $I > 2\sigma(I)$ and 453 refinement parameters. The absolute structure parameter is –0.01(4).

Synthesis of 1-[2-(4-chlorophenylthio)acetyl]-5-(methoxycarbonyl)-2-phenylpyrrolidine-3-carboxylic acids 7a,c (general procedure). Through a solution of 4-*tert*-butyl ester of substituted pyrrolidine-2,4-dicarboxylic acid **6** (2.0 mmol) in anhydrous $CHCl_3$ (30 mL), gaseous HCl was passed for 2 h and the solution was stirred at room temperature for 24 h. Then, 5 mL of saturated $NaHCO_3$ solution was added to pH 5, the organic phase of the washed with saturated NaCl solution, dried with Na_2SO_4, and the solvents were evaporated *in vacuo*. The product was purified by recrystallization from Et_2O—MeOH, 20 : 1.

(2*R,3*S**,5*S**)-1-[2-(4-Chlorophenylthio)acetyl]-5-(methoxycarbonyl)-2-phenylpyrrolidine-3-carboxylic acid (7a).** The yield was 87%, colorless crystals, m.p. 189—190 °C. ^{1}H NMR (DMSO-d_6, δ, *J*/Hz): 2.20 (q, 1 H, H(4), *J* = 12.5); 2.34 (dt, 1 H, H(4), *J* = 12.5, *J* = 6.5); 3.23 (d, 1 H, CH_2S, *J* = 15.9); 3.62 (ddd, 1 H, H(3), *J* = 12.5, *J* = 8.9, *J* = 6.5); 3.71 (s, 3 H, $COOCH_3$); 3.96 (d, 1 H, CH_2S, *J* = 15.9); 4.36 (dd, 1 H, H(5), *J* = 11.3, *J* = 6.8); 5.34 (d, 1 H, H(2), *J* = 8.9); 7.08 (d, 1 H, 2 H_{arom}, *J* = 8.6); 7.26—7.32 (m, 3 H_{arom}); 7.37 (t, 2 H_{arom}, *J* = 7.5); 7.64 (d, 2 H_{arom}, *J* = 7.5); 12.48 (br.s, COOH). ^{13}C NMR (DMSO-d_6, δ): 29.00, 36.41, 49.40, 52.49, 59.64, 62.68, 128.28 (2 C), 128.43, 128.70 (2 C), 129.17 (2 C), 129.79 (2 C), 130.86, 135.29, 138.99, 167.11, 170.63, 172.29. Found (%): C, 58.05; H, 4.71; N, 3.02. $C_{21}H_{20}ClNO_5S$. Calculated (%): C, 58.13; H, 4.65; N, 3.23.

(2*R,3*S**,5*S**)-1-[2-(4-Chlorophenylthio)acetyl]-5-(methoxycarbonyl)-5-methyl-2-phenylpyrrolidine-3-carboxylic acid (7c).** The yield was 94%, colorless crystals, m.p. 108—109 °C. ^{1}H MR (DMSO-d_6, δ, *J*/Hz): 1.48 (s, 3 H, 2-CH_3); 1.95 (dd, 1 H, H(4), *J* = 12.4, *J* = 6.2); 2.46—2.53 (m, 1 H, H(4)); 3.09 (d, 1 H, CH_2S, *J* = 15.7); 3.69 (s, 3 H, $COOCH_3$); 3.74 (d, 1 H, CH_2S, *J* = 15.7); 3.81 (ddd, 1 H, H(3), *J* = 13.6, *J* = 9.0, *J* = 6.2); 5.50 (d, 1 H, H(2), *J* = 9.0); 7.02—7.06 (m, 2 H_{arom}); 7.25—7.29 (m, 3 H_{arom}); 7.33—7.37 (m, 2 H_{arom}); 7.64—7.66 (m, 2 H_{arom}). ^{13}C NMR (DMSO-d_6, δ): 20.62, 36.85, 37.19, 48.88, 52.70, 62.99, 66.28, 128.31, 128.45 (2 C), 128.69 (2 C), 129.15 (2 C), 129.92 (2 C), 130.91, 135.11, 139.53, 165.90, 171.04, 173.71. Found (%): C, 59.17; H, 4.92; N, 3.30. $C_{22}H_{22}ClNO_5S$. Calculated (%): C, 58.99; H, 4.95; N, 3.13.

This work was financially supported by the Russian Foundation for Basic Research (Project Nos 11-03-00630-a, 11-03-91375-ST_a and 08-04-01800-a).

References

1. A. A. Butylin, M. A. Panteleev, F. I. Ataullakhanov, *Ros. Khim. Zhurn.* (*Zh. Ros. Khim. O-va im. D. I. Mendeleeva*), 2007, **LI**, 45 [*Mendeleev Chem. J.* (*Engl. Transl.*), 2007, **51**].
2. N. Mackman, *Nature*, 2008, **451**, 914.
3. B. Hughes, *Nature Rev. Drug Discovery*, 2010, **9**, 903.
4. E. Schweizer, A. Hoffmann-Roder, J. A. Olsen, P. Seiler, U. Obst-Sander, B. Wagner, M. Kansy, D. W. Banner, F. Diederich, *Org. Biomol. Chem.*, 2006, **4**, 2364.
5. B. Baum, M. Mohamed, M. Zayed, C. Gerlach, A. Heine, D. Hangauer, G. Klebe, *J. Mol. Biol.*, 2009, **390**, 56.
6. Y. N. Imai, Y. Inoue, I. Nakanishi, K. Kitaura, *Protein Science*, 2008, **17**, 1129.
7. K. V. Kudryavtsev, M. Yu. Tsentalovich, A. S. Yegorov, E. L. Kolychev, *J. Heterocyclic Chem.*, 2006, **43**, 1461.
8. K. V. Kudryavtsev, *Zh. Org. Khim.*, 2010, **46**, 379 [*Russ. J. Org. Chem.* (*Engl. Transl.*), 2010, **46**, 372].
9. T. A. Halgren, *J. Comp. Chem.*, 1996, **17**, 490.
10. R. Guha, M. T. Howard, G. R. Hutchison, P. Murray-Rust, H. Rzepa, C. Steinbeck, J. K. Wegner, E. Willighagen, *J. Chem. Inf. Model.*, 2006, **46**, 991.
11. M. F. Sanner, *J. Mol. Graphics Mod.*, 1999, **17**, 57.
12. Yu. Lu, T. Shi, Y. Wang, H. Yang, X. Yan, X. Luo, H. Jiang, W. Zhu, *J. Med. Chem.*, 2009, **52**, 2854.
13. G. M. Sheldrick, *Acta Crystallogr., Sect. A*, 2008, **64**, 112.
14. Ya. N. Kotova, E. A. Kostanova, M. A. Rozenfel´d, E. I. Sinauridze, M. A. Panteleev, F. I. Ataullakhanov, *Biologicheskie Membrany* [*Biological Membranes*], 2009, **26**, 514 (in Russian).
15. O. Tsuge, S. Kanemasa, M. Yoshioka, *J. Org. Chem.*, 1988, **53**, 1384.
16. K. V. Kudryavtsev, A. A. Zagulyaeva, *Zh. Org. Khim.*, 2008, **44**, 384 [*Russ. J. Org. Chem.* (*Engl. Transl.*), 2008, **44**, 378].

Received March 15, 2011;
in revised form April 11, 2011